Numerical and Experimental Analyses of Added Resistance in Waves

by Yonghwan Kim*, Min-Guk Seo, Dong-Min Park, Jae-Hoon Lee. Kyung-Kyu Yang

Department of Naval Architecture & Ocean Engineering, Seoul National University, Seoul, Korea

E-mail: *yhwankim@snu.ac.kr*

Highlights:

- Different numerical methods and formulations are applied to the prediction of added resistance, and their results are compared each other and also with experimental data for validation.
- Towing-tank experiments are carried out for the ships with different bow shapes and their added resistance are compared. Uncertainty analysis is carried out for the added resistance experiment.
- Added resistance in short waves is compared between experiment, numerical computation, and empirical and asymptotic formulae. Their differences are introduced.

1. Introduction

Recently the discussions at the International Maritime Organization (IMO) have resulted in the development of an Energy Efficiency Design Index (EEDI) to measure how much greenhouse gas a ship emits, and to restrict greenhouse gas emissions from ships. For these reasons, ship designers should find optimum hull forms to minimize resistance in ocean waves, and pay great attention to the added resistance problem.

This study considers a systematic study on added resistance problem by using numerical and experimental approaches. Particularly this study includes the most existing methods for numerical methods, including strip method, 3D panel method, and CFD. Both direct pressure integration and far-field formulae are applied for the computation of added resistance. The present study includes a series of towing-tank experiment. By comparing the computed and measured results, both results are validated each other. The present study includes the observation on the effects of bow shapes on added resistance and the uncertainty analysis in added resistance experiment.

2. Computational Methods

In the present study, three numerical methods are applied to the computation of added resistance: strip method based on STF method, 3D Rankine panel method, and a Cartesian-grid-based Euler solver. The below describes a very brief summary of the formulations for seakeeping and added resistance. The details and notions are in the paper of Seo *et al.(*2013).

2.1 Strip Method

Salvensen-Tuck-Faltinsen method(1980) is applied as the method of solution for seakeeping analysis. For the sectional BVPs of sway, heave and roll motions, 2D wave Green function is computed by using NIIRID code developed at MIT. The added resistance can be computed by using three formulations:

- Near-field formulation (Faltinsen, 1980)

$$R = \int_C \left\{ -\frac{\rho g}{2} \overline{\zeta_r^{\,2}} \right\} n_1 ds - \omega_e^{\,2} M \overline{\xi_3 \xi_5^{\,*}} + \omega_e^{\,2} M \overline{(\xi_2 - z_G \xi_4)\xi_5^{\,*}} + \rho \int_{S_B} \left\{ (\xi_2 + x\xi_6 - z\xi_4\eta_4) \frac{\partial}{\partial y}\left(\frac{\partial \phi}{\partial t} + U\frac{\partial \phi}{\partial x}\right)\Big|_m + (\xi_2 + x\xi_6 - z\xi_4\eta_4) \frac{\partial}{\partial y}\left(\frac{\partial \phi}{\partial t} + U\frac{\partial \phi}{\partial x}\right)\Big|_m + \frac{1}{2}\left(\left(\frac{\partial \phi}{\partial x}\right)^2 + \left(\frac{\partial \phi}{\partial y}\right)^2 + \left(\frac{\partial \phi}{\partial z}\right)^2 \right) \right\} n_1 ds \rho \tag{1}$$

- Far-field formulation (Maruo, 1960)

$$R = \frac{\rho k^2}{8\pi} \int_0^{2\pi} \left| H(\theta) \right|^2 \left(\cos\theta + \cos\beta \right) d\theta \tag{2}$$

- Energy-rated formulation (Salvesen,

$$R = -\frac{i}{2} k \cos\beta \sum_{j=3,5} \xi_j \left\{ (F_j^{\,I})^* + F_j^{\,D} \right\} - \frac{1}{2} \zeta_I^{\,2} \frac{\omega^2}{\omega_e} k \cos\beta \int_L e^{-2kds} (b_{33} + b_{22} \sin^2\beta) dx \tag{3}$$

2.2 3D Time-Domain Rankine Panel Method

A time-domain Rankine panel method is applied to the linear and nonlinear seakeeping problem and resultant added resistance computation. In past years, WISH program has been developed at Seoul National University, and many

variations are created for various seakeeping problems of ships and offshore structures. In this method, the velocity potential is decomposed into three components: basis, incident, and disturbed components, Φ , ϕ_I , ϕ_d , respectively. Then, Green's theorem is solved by using B-spline basis functions for potential, wave elevation, and normal potential on hull and free surface.

In this method, three levels of nonlinear formulations are applied. Linear (WISH 1), weakly nonlinear (WISH 2), and weak-scattered (WISH 3) formulations are applied for linear and nonlinear computations. For linear and weakly nonlinear formulations, added resistance can be computed by using two approaches: near- and far-field methods. In the case of weak-scatterer formulation, direct pressure integration should be applied.

- Near-field formulation

$$\begin{aligned}\vec{F}_2 &= \int_{WL} \frac{1}{2}\rho g\left(\zeta-(\xi_3+\xi_4 y-\xi_5 x)\right)^2\cdot\vec{n}\,dL-\rho\int_{WL}\left(-(\vec{U}-\frac{1}{2}\nabla\Phi)\cdot\nabla\Phi\right)\left(\zeta-(\xi_3+\xi_4 y-\xi_5 x)\right)\cdot\vec{n}_1\,dL\\ &-\rho\int_{WL}\vec{\delta}\cdot\nabla\left(-(\vec{U}-\frac{1}{2}\nabla\Phi)\cdot\nabla\Phi\right)\left(\zeta-(\xi_3+\xi_4 y-\xi_5 x)\right)\cdot\vec{n}\,dL-\rho\iint_{\bar{S}_B} gz\cdot\vec{n}_2\;ds\\ &-\rho\iint_{\bar{S}_B}\frac{1}{2}\left(\nabla\left(\phi_I+\phi_d\right)\cdot\nabla\left(\phi_I+\phi_d\right)\right)\cdot\vec{n}\;ds-\rho\iint_{\bar{S}_B}\vec{\delta}\cdot\nabla\left(\frac{\partial\left(\phi_I+\phi_d\right)}{\partial t}-\left(\vec{U}-\nabla\Phi\right)\cdot\nabla\left(\phi_I+\phi_d\right)\right)\cdot\vec{n}\;ds\\ &-\rho\iint_{\bar{S}_B}\left(g(\xi_3+\xi_4 y-\xi_5 x)+\frac{\partial\left(\phi_I+\phi_d\right)}{\partial t}-\left(\vec{U}-\nabla\Phi\right)\cdot\nabla\left(\phi_I+\phi_d\right)\right)\cdot\vec{n}_1\;ds\\ &-\rho\iint_{\bar{S}_B}\left[\left(-(\vec{U}-\frac{1}{2}\nabla\Phi)\cdot\nabla\Phi\right)\cdot\vec{n}_2\right]ds-\rho\iint_{\bar{S}_B}\vec{\delta}\cdot\nabla\left(-(\vec{U}-\frac{1}{2}\nabla\Phi)\cdot\nabla\Phi\right)\cdot\vec{n}_1\;ds\end{aligned} \tag{4}$$

- Far-field formulation(momentum conservation)

$$\begin{aligned}\vec{F}_2 &= \frac{1}{2}\rho\int_{C_d}\frac{\left(\nabla(\phi_I+\phi_d)\cdot\nabla(\phi_I+\phi_d)+k^2(\phi_I+\phi_d)^2\right)}{2k}\vec{n}_c dL-\rho\int_{C_d}\frac{\nabla(\phi_I+\phi_d)\left(\nabla(\phi_I+\phi_d)\cdot\vec{n}_c\right)}{2k}dL-\frac{\rho g}{2}\int_{C_d}(\zeta_I+\zeta_d)^2\vec{n}_c dL\\ &-\rho\int_{C_d}\left[\nabla\Phi(\nabla(\phi_I+\phi_d)\cdot\vec{n}_c)+\nabla(\phi_I+\phi_d)(\nabla\Phi\cdot\vec{n}_c)\right](\zeta_I+\zeta_d)dL\end{aligned} \tag{5}$$

2.3 Cartesian-Grid-Based Euler Solver

A finite-volume method is applied for CFD-based computation. Particularly, this study focuses on the Euler equation since seakeeping and added resistance are inertia-dominant problems. Then the following governing equations are solved using a Cartesian-grid-based approach:

$$\int_\Gamma\left(\vec{u}\cdot\vec{n}\right)dS=0 \qquad \text{and} \qquad \frac{\partial}{\partial t}\int_\Omega\vec{u}dV+\int_\Gamma\vec{u}\left(\vec{u}\cdot\vec{n}\right)dS=\frac{1}{\rho}\left[-\int_\Gamma p\vec{n}dS+\int_\Omega\vec{f}_b dV\right] \tag{6}$$

The governing equations are solved by adopting a fractional step method, and THINC and WLIC free-surface interface are applied to track the free-surface interface (Yang *et al*., 2013) Level-set approach is implemented complex ship surface. Added resistance can be computed by using direct pressure integration, and subtracting the resistance in calm water from the total force on ship in waves.

2.4 Added Resistance in Short Waves

Added resistance in short waves is of great interest due to the poor prediction of linear-based formulation of numerical computation. To overcome such problem, some formulae have been proposed as follows:

- Faltinsen (1980)

$$\overline{\vec{F}_2}=\int_L\frac{1}{2}\rho g\zeta_I^2\left[\sin^2(\theta-\beta)+\frac{2\omega U}{g}\left[1+\cos\theta\cos(\theta-\beta)\right]\right]\vec{n}dL \tag{7}$$

- Fujii & Takahashi (1975) and Kuroda et al. (2008)

$$R=\alpha_d(1+\alpha_U)\left[\frac{1}{2}\rho g\zeta_I^2 BB_f(\beta)\right] \tag{8}$$

$$B_f(\beta)=\frac{1}{B}\left[\int_I\sin^2(\theta-\beta)\sin\theta dl+\int_{II}\sin^2(\theta+\beta)\sin\theta dl\right],\quad \alpha_d=\frac{\pi^2 I_1^2(kd)}{\pi^2 I_1^2(kd)+K_1^2(kd)}\;,\quad \alpha_U=5\sqrt{F_n}\quad \text{(F \& T)} \tag{9}$$

$$B_f(\beta) = \frac{1}{B}\left[\int_I \sin^2(\theta-\beta)\sin\theta dl + \int_{II} \sin^2(\theta+\beta)\sin\theta dl\right]$$

$$\alpha_d = \frac{\pi^2 I_1^2(k_e d)}{\pi^2 I_1^2(k_e d) + K_1^2(k_e d)}, \left(k_e = \frac{\omega_e^2}{g}\right), \quad \alpha_U = C_U F_n, \quad \left(C_U = \max[10.0, -310 B_f(\beta) + 68]\right) \qquad \text{(Kuroda)} \qquad (10)$$

3. Towing-Tank Experiment

In the present study, a series of experiment are carried out at the towing tank of Seoul National University. In head seas, the time signals of heave-roll-pitch motions and added resistance are measured. Surge motion is set to be free, and wave probes are located at a fixed location in towing tank and also with moving carriage. Resistance in still water is measured before the test in waves, so that the added resistance quantities are obtained by subtracting the resistance in still water to the total forces in waves.

Uncertainty analysis is carried out for seakeeping and added resistance experiment at three wave conditions. More than fifteen tests are repeated and the uncertainty analysis is based on ITTC's Guidance and Procedure (2008) which adopts the method of ISO(1995). Seven primary sources of uncertainty are categorized, and the Type A and B uncertainties are analyzed.

4. Results

Fig. 1 shows the added resistance on S175 hull. As this result shows, computational results show good overall correspondence with existing experimental data, but some differences can be found in peaks between computational results. Also computational methods underpredict in short waves. According to our study, the agreement of computational results with experiment depends on the slenderness of ship and speed. Particularly the grid dependency test is essential in Rankine panel method and CFD-based computation. In the case of strip theory, overall agreement is not as good as 3D methods, but it may be practically acceptable if empirical formula is combined for short waves.

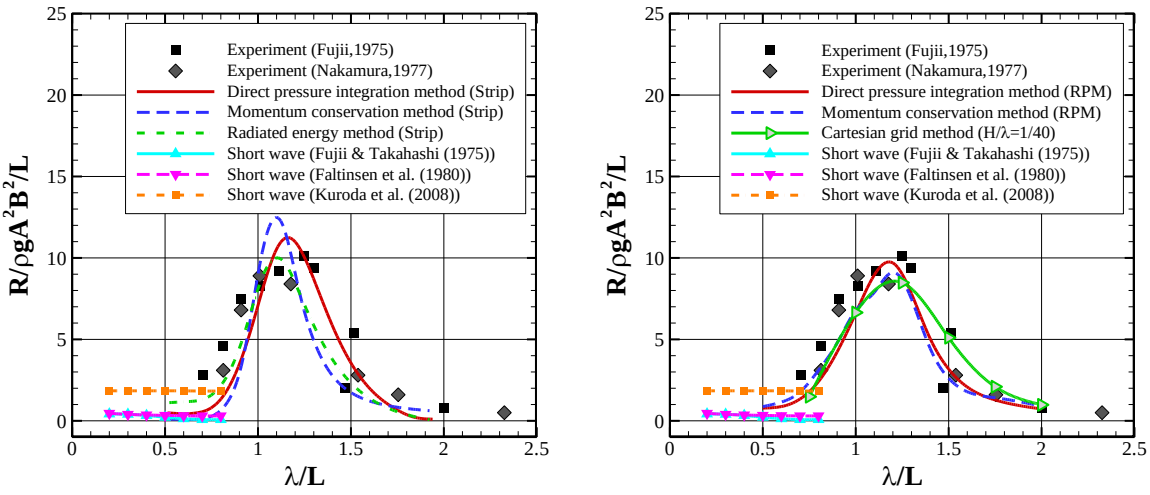

(a) Strip method (b) Rankine panel method and Cartesian grid method

Fig. 1 Comparison of added resistance on S175: Fn = 0.25

Fig. 2 shows an example of grid dependency in CFD computation for KVLCC2 tanker. In this figure, it is obvious that the grids resolution along ship length, particularly near bow region, is critical for short waves. Since diffraction around bow plays a key role in short waves, capturing appropriate wave profile near bow is very important.

Prediction of the effects of bow shape on added resistance is of great interest for ship design. Fig. 3 shows three types of bow shapes for KVLCC2. In the case of Ax-bow, hull geometry above still level is modified, while the whole bow shape is modified in the case of leadge bow. The measured data of added resistance are plotted in Fig. 4. The modified KVLCC2 hulls with both Ax-bow and leadge bow show less quantities than those of original bow shape. Particularly the reduction of leadge bow is slightly larger than Ax-bow.

In the case of experiment, understanding the amount of error is important. However, any uncertainty analysis has not been introduced yet. In this study, a thorough uncertainty analysis is performed for three wave conditions and the amounts of errors are observed. For example, Fig. 5 shows the main sources and their contributions to error are summarized. According to this result, the accuracy of all three measurements, i.e. resistance in waves and also in still water, and wave amplitude, are important. Especially, in this study, it is found that type B uncertainty, i.e. uncertainty in device and calibration, takes the uncertainty larger than type A uncertainty which is from the repeated test.

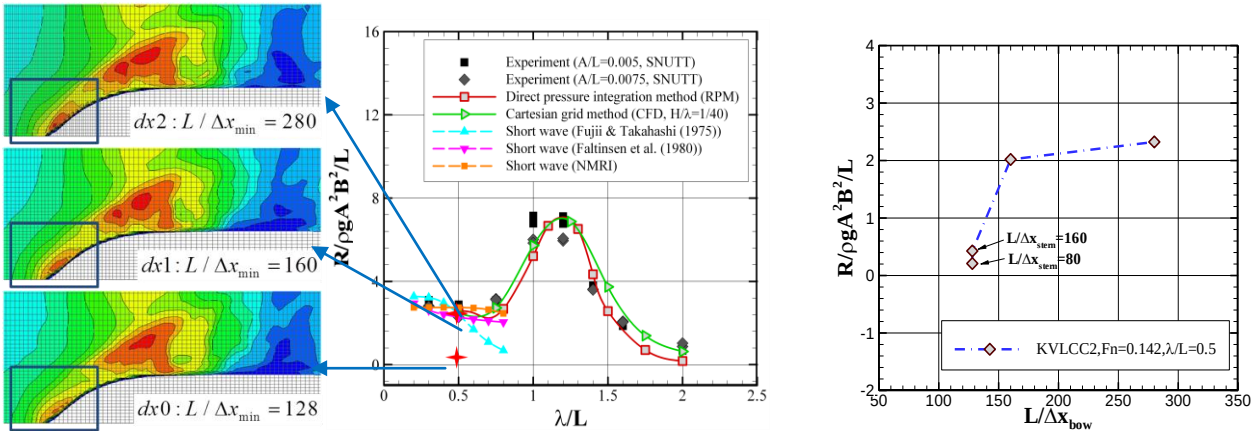

Fig. 2 Grid dependency in show waves: KVLCC2 hull, Fn=0.142, A/ λ = 1/80

(a) Original (above) and Ax-bow (below) of KVLCC2 (b) Modified KVLCC2 with leadge bow

Fig. 3 Hull forms of KVLCC2 tanker with three different bow shapes

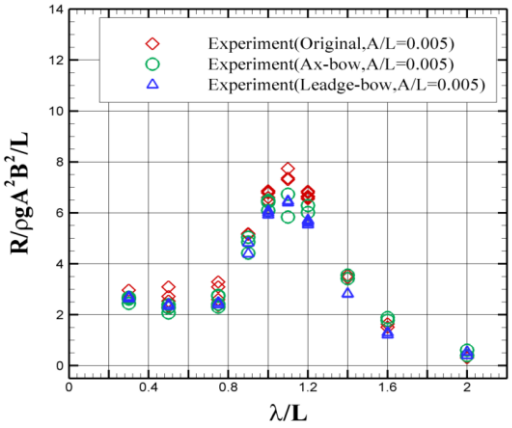

Fig. 4 Comparison of added resistance for three bow shapes: KVLCC2, Fn=0.142

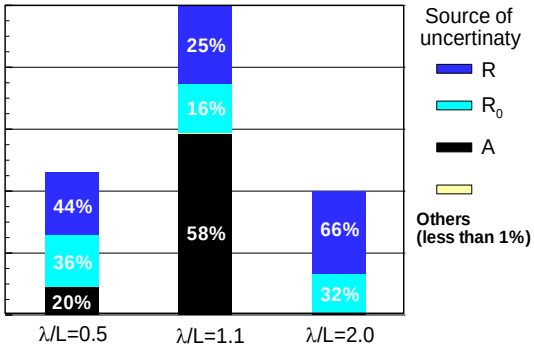

Fig. 5 Main sources of uncertainty in added resistance experiment: KVLCC2, Fn=0.142 (R: measured resistance in waves, Ro: measured resistance in still water, A: measured wave amplitude)

References

Faltinsen, O.M., Minsaas, K.J., Liapis, N., Skjørdal, S.O., 1980. Prediction of resistance and propulsion of a ship in a seaway. In: Proceedings of the 13th symposium on naval hydrodynamics. Tokyo, Japan.

Kim, K.H., Kim, Y., 2011. Numerical study on added resistance of ships by using a time-domain Rankine panel method. Ocean Eng. 38, 1357-1367.

Kuroda, M., Tsujimoto, M., Fujiwara, T., Ohmatsu, S., Takagi, K., 2008. Investigation on components of added resistance in short waves. J. Jpn. Soc. Nav. Archit. Ocean Eng. 8, 171-176.

Maruo, H., 1960. The drift of a body floating on waves. J. Ship Res. 4 (3), 1-10.

Matsumoto, K., Hirota, K., Takagishi, K., 2000. Development of energy saving bow shape at sea, 4th Osaka Colloq. Seakeeping and Stability of Ships, Osaka.

Ohihara, H., Matsumoto, K., Yamasaki, K., Takagishi, K., 2008. CFD Simulation for development of high-performance hull forms in a seaway, 6th Osaka Colloq. Seakeeping and Stability of Ships, Osaka.

Seo, M.G., Park, D.M., Yang, K.K., Kim, Y., 2013. Comparative study on computation of ship added resistance in waves. Ocean Eng. 73, 1-15.

Yang, K.K., Nam, B.W., Lee, J.H., Kim, Y., 2013. Numerical Analysis of Large-Amplitude Ship Motions Using FV-based Cartesian Grid Method. Int. J. Offshore Polar Eng. 23 (3), 186-196.